



OPEN ACCESS

EDITED BY

Maria Mavroulidou,
London South Bank University,
United Kingdom

REVIEWED BY

Shenghua Lv,
Shaanxi University of Science and
Technology, China
Nitish Venkateswarlu Mogili,
National Institute of Technology, Andhra
Pradesh, India

*CORRESPONDENCE

Kazunori Nakashima,
✉ k.naka@eng.hokudai.ac.jp

RECEIVED 30 September 2023

ACCEPTED 05 December 2023

PUBLISHED 08 January 2024

CITATION

Nawarathna THK, Sakai J, Nakashima K,
Kawabe T, Shikama M, Takano C and
Kawasaki S (2024), Combination of
cellulose nanofiber and artificial fusion
protein for biocementation.
Front. Built Environ. 9:1305003.
doi: 10.3389/fbuil.2023.1305003

COPYRIGHT

© 2024 Nawarathna, Sakai, Nakashima,
Kawabe, Shikama, Takano and Kawasaki.
This is an open-access article distributed
under the terms of the [Creative
Commons Attribution License \(CC BY\)](#).
The use, distribution or reproduction in
other forums is permitted, provided the
original author(s) and the copyright
owner(s) are credited and that the original
publication in this journal is cited, in
accordance with accepted academic
practice. No use, distribution or
reproduction is permitted which does not
comply with these terms.

Combination of cellulose nanofiber and artificial fusion protein for biocementation

Thiloththama Hiranya Kumari Nawarathna^{1,2}, Jin Sakai²,
Kazunori Nakashima^{3*}, Tetsuya Kawabe², Miki Shikama²,
Chikara Takano³ and Satoru Kawasaki³

¹Department of Engineering Technology, Faculty of Technology, University of Jaffna, Kilinochchi, Sri Lanka, ²Division of Sustainable Resources Engineering, Graduate School of Engineering, Hokkaido University, Sapporo, Japan, ³Division of Sustainable Resources Engineering, Faculty of Engineering, Hokkaido University, Sapporo, Japan

Biomineralization occurring in living organisms is mostly controlled by organic macromolecules such as polysaccharides and proteins. Recently, biomineralization has been attracting much attention as a green and sustainable cementation technique including enzyme-induced carbonate precipitation (EICP), where CaCO_3 is formed by hydrolysis of urea by urease in the presence of calcium ions. In this study, we have developed a novel hybrid biocementation method combining CaCO_3 and cellulose nanofiber (CNF). In nature, matrix proteins work as a binder at the interface of organic and inorganic materials to form hybrid biomaterials. By mimicking the natural system, we designed an artificial fusion protein to facilitate the deposition of CaCO_3 on CNF. Calcite-binding peptide (CaBP) and carbohydrate-binding module (CBM) were introduced in the artificial fusion protein CaBP-CBM to connect CaCO_3 and cellulose. The addition of CNF in the EICP system resulted in the formation of a number of small particles of CaCO_3 compared to a non-additive system. The addition of the fusion protein CaBP-CBM to CNF led to an increase in the size of CaCO_3 particles. Furthermore, the combination of CaBP-CBM and CNF provides higher strength of samples in sand solidification. Therefore, introduction of CNF and the fusion protein would be promising for novel biocementation techniques.

KEYWORDS

biocement, cellulose nanofiber, fusion protein, hybrid materials, calcium carbonate

1 Introduction

Biomineralization-inspired materials gained much attention recently in various fields as environmentally friendly and sustainable green composite materials (Saito et al., 2014; Kuo et al., 2018; Nawarathna et al., 2021). In biomineralization, the organic matrix plays a vital role and controls the nature, morphology, and orientation of the mineral phase (Dalas et al., 2000). Generally, the organic matrix of biominerals contains polysaccharides such as chitin and cellulose and inorganic materials such as calcium carbonate (CaCO_3), calcium phosphate, hydroxyapatite, and silicate (Dalas et al., 2000; Kuo et al., 2018). Neutral pH and ambient temperature are most suitable for the formation of biominerals, and compared with the non-biogenic minerals, biominerals show higher mechanical strength (Arakaki et al., 2015). Calcium carbonate in molluscan shells (Stephen and Lia, 1997), hydroxyapatite in the bones and teeth of mammals (Dorozhkin and Epple, 2002), and silica

in diatoms (Chambers et al., 1999) are some good examples for biomineral formation in nature.

Among the biominerals, CaCO_3 is abundant in most of organisms, and this biogenic CaCO_3 exhibits excellent optical and mechanical properties (Shi et al., 2022). The nacre of mollusk shells consists of an organic/inorganic layered structure where aragonite CaCO_3 has been deposited on chitin sheets to form a tough and hard structure (Jackson et al., 1990). In the exoskeletons of crustaceans, amorphous CaCO_3 is formed in the chitin matrix with the assistance of matrix proteins. This composite makes the exoskeletons of crustaceans flexible, tough, and transparent (Kuo et al., 2018).

Matrix proteins play an important role during the formation of biogenic CaCO_3 on the organic matrix. In nature, different kinds of proteins have been assisted for efficient formation of organic- CaCO_3 hybrid materials (Sudo et al., 1997; Suzuki et al., 2009; Inoue et al., 2014). In the exoskeleton of the crayfish, the acidic protein CAP-1 is involved in the efficient formation of CaCO_3 on chitin (Sugawara et al., 2006). In addition to the binding property of CAP-1 to chitin, it promotes CaCO_3 formation due to the presence of seven acidic amino acids at the C-terminus (Rebers and Riddiford, 1988; Sugawara et al., 2006). Similarly, several other matrix proteins have been identified from the mantle of *Hemitoma cumingii* (Jin et al., 2019), pearl oyster (Nakayama et al., 2013), nacreous layer of *Pinctada margaritifera* (Montagnani et al., 2011) etc., which support the formation of CaCO_3 on chitin. Due to the associated higher strength, fracture resistance, and toughness of biominerals, today, researchers have taken steps to synthesize CaCO_3 -organic hybrid materials by mimicking the concept of biomineral formation for different industrial applications.

In our previous research, by mimicking the nature, an artificial fusion protein was developed for the efficient precipitation of CaCO_3 on chitin to accelerate the efficiency of the enzyme-induced biocementation process (Nawarathna et al., 2021). Enzyme-induced carbonate precipitation (EICP) is a novel, sustainable, and eco-friendly bio-cementation method where biogenic CaCO_3 is produced by bio-geochemical reactions stimulated by the enzyme urease. Urease is a nickel-containing enzyme (Maroney and Ciarli, 2014) which has the capability to hydrolyze urea into ammonia and bicarbonate ions. Under the alkaline condition, in the presence of calcium ions, CaCO_3 is produced (DeJong et al., 2006; Whiffin et al., 2007; Gowthaman et al., 2019). It has been proven that this biogenic CaCO_3 can work as a better bio-cementing material (DeJong et al., 2006; Whiffin et al., 2007; Gowthaman et al., 2019). The efficiency of the process and properties of the bio-cement can be further improved by introducing organic materials into the process (Hamdan et al., 2016; Zhao et al., 2016). However, having the matrix protein at the interface of organic and inorganic materials provides a better binding between the organic and inorganic materials and forms excellent hybrid materials.

In this research, an artificial recombinant protein was developed to produce an organic-inorganic hybrid green material by efficient formation of CaCO_3 on the cellulose biopolymer. Same as chitin, cellulose is one of the most abundant, biodegradable, non-toxic, and highly crystalline natural polysaccharide mainly derived from biomass (Kramar and González-Benito, 2022; Ezquerro et al., 2023). It is a linear polymer containing D-glucopyranose units linked via the β -1-4 glycoside bond (Klemm et al., 2005).

Cellulose nanomaterials are extensively used in different fields such as food packaging, drug delivery, in biomedical materials, sensor, biodegradable plastics, and composites (Klemm et al., 2005; Vilela et al., 2010). Nowadays, cellulose- CaCO_3 composites have gained much attention, especially in bio-medical applications and also in protective packaging and flexible display panels with high impact resistance (Saito et al., 2014).

In this research, a cellulose- CaCO_3 composite was produced by using the EICP process with cellulosic materials. An artificial fusion protein CaBP-CBM composed of calcite-binding peptide (CaBP) and carbohydrate-binding module (CBM) was developed in order to achieve efficient precipitation of CaCO_3 on the cellulose matrix (Figure 1). Here, the carbohydrate-binding module (CBM3) from *Clostridium thermocellum* (Hong et al., 2007) and CaBP with a short sequence (Sarikaya et al., 2003) were used to fabricate the fusion protein. CBM3 has a great ability to bind to cellulosic materials (Mwandira et al., 2020), and CaBP has an ability to bind to CaCO_3 (Sarikaya et al., 2003). The effect of the recombinant protein on CaCO_3 crystallization and formation of the cellulose- CaCO_3 composite was analyzed. Furthermore, the effects of the produced bio-composite material on sand densification were examined by using urease-mediated biocementation.

2 Materials and methods

2.1 Materials

The synthetic gene of calcite-binding peptide (CaBP: DVFSSFNLKHMR) derived from the phage-display system (Sarikaya et al., 2003) was purchased from GenScript (Tokyo, Japan). The carbohydrate-binding module, CBM3 (hereafter named as CBM), from *Clostridium thermocellum* (Accession, Q06851) (Hong et al., 2007; Mwandira et al., 2020; Togo et al., 2020) optimized for the expression in *E. coli* was purchased from Eurofins Genomics (Tokyo, Japan). Tryptone and yeast extract were purchased from BD Biosciences Advanced Bioprocessing (Miami, FL, United States). Ampicillin and isopropyl β -D-thiogalactopyranoside (IPTG) were obtained from Nacalai Tesque (Tokyo, Japan). Cellulose nanofiber (CNF, product name: nanoforest-S) was purchased from Chuetsu Pulp & Paper Co., Ltd. (Takaoka, Japan). All other organic materials and chemical reagents were purchased from Wako Pure Chemical Industries Ltd.

2.2 Gene construction and protein expression

The structure of the fusion protein CaBP-CBM prepared in this research is shown in Figure 1A. The vector construction for CaBP-CBM was conducted in a similar manner as in our previous study (Nawarathna et al., 2021). Briefly, the gene for CaBP was introduced at the N-terminal region of the CBM gene by the polymerase chain reaction (PCR) using PrimeSTAR Max DNA polymerase (Takara Bio, Japan). The pET-15b vector (Novagen) was linearized using Nde I and Xho I restriction enzymes (New England Bio Labs, Japan), and the amplified CaBP-CBM gene was inserted by the In-Fusion system (Takara Bio) to construct the expression vector pET15-

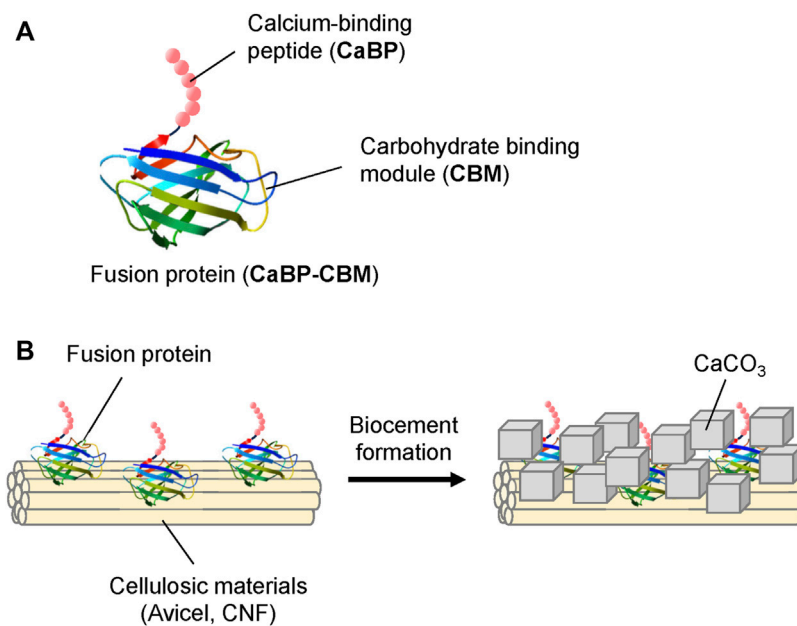


FIGURE 1

(A) Structure of the fusion protein (CaBP-CBM). (B) Conceptual illustration of CaCO₃ formation on cellulosic materials.

CaBP-CBM. Here, restriction enzyme sites were selected to include a His-tag at the N-terminus of CaBP-CBM. *E. coli* BL21 (DE3) was transformed with pET15-CaBP-CBM and cultured at 37°C and 160 rpm in LB-Amp medium until the OD₆₀₀ attained a value of 0.5. Then, protein expression was induced by adding 0.5 mM IPTG and shaking at 30°C and 160 rpm for 24 h. By centrifugation of the cell suspension (8000 × g, 4°C, 10 min), bacteria cells were harvested and re-suspended in lysis buffer. The cell lysate was obtained by disruption of the cells using ultrasonication (VCX-130, Sonics & Materials Inc., United States; strength: 30%, 2 min). Then, the cell debris was removed by centrifugation (4°C, 12,000 × g, 20 min) of the lysate. Since SDS-PAGE (Atto Company Limited, Tokyo, Japan) has confirmed that the protein was expressed as a soluble protein, purification of the protein was done by His-tag purification using Bio-Scale Mini Nuvia IMAC Cartridges (Bio-Rad Laboratories, Inc., Tokyo, Japan). The purified protein was concentrated using Amicon Ultra-4 (10 kDa), and then the buffer was replaced with Tris-HCl (pH 9).

2.3 Cellulose-binding assay

The ability of the fusion protein CaBP-CBM to bind to microcrystalline Avicel and cellulose nanofiber (CNF) was investigated. Cellulosic materials (15 mg/mL) were mixed with CBM (265 µg/mL) in 50 mM Tris-HCl buffer (pH 9) and shaken at 25°C. To measure the rate of binding of the fusion protein to cellulosic materials, samples were collected at different time intervals (0, 5, 10, 30, 60, and 120 min). The supernatant of the collected samples was obtained by centrifugation (13,000 × g, 10 min). To calculate the adsorption of the fusion protein on cellulosic materials, the protein concentration of the supernatant was measured.

2.4 Effect of additives on CaCO₃ precipitation by the urease enzyme

The calcium carbonate (CaCO₃) precipitation experiment was conducted with different additives by using the urease-induced carbonate precipitation method. Urease can hydrolyze urea to produce ammonia and bicarbonate ions. In the presence of calcium ions, bicarbonate ions instantaneously give calcium carbonate (CaCO₃). The process is induced by the generated ammonia (Nawarathna et al., 2019). Extracted jack bean urease (2.5 U/mL, Wako Pure Chemical Industries Ltd., Tokyo, Japan) was used for the experiments with 0.75 mol/L of CaCl₂ and 0.75 mol/L of urea. The same concentration of cellulosic material (3.8 mg/mL) used for the adsorption test was selected for the precipitation test, while the fusion protein concentration (66 µg/mL) was selected independently. Specimens were prepared without the protein, with fusion protein (66 µg/mL), with CNF or microcrystalline Avicel (3.8 mg/mL), and with both CNF/microcrystalline Avicel (3.8 mg/mL) and fusion protein (66 µg/mL). The reaction mixture was kept in the shaking incubator for 24 h at 25°C and 160 rpm, and the precipitate was separated from the supernatant by centrifugation (24°C, 12,000 rpm, 10 min). The precipitate was washed with distilled water and freeze-dried. Morphology and polymorphs of the precipitated CaCO₃ were analyzed by using scanning electron microscopy (SEM; Miniscope TM3000, Hitachi, Tokyo, Japan) and X-ray diffraction (XRD; MultiFlex, Rigaku Co., Ltd., Tokyo, Japan).

2.5 Sand solidification by urease-producing bacteria

A sand solidification experiment was conducted for oven-dried (110°C for 2 days) Mikawa silica sand (No. 4) by using microbial-

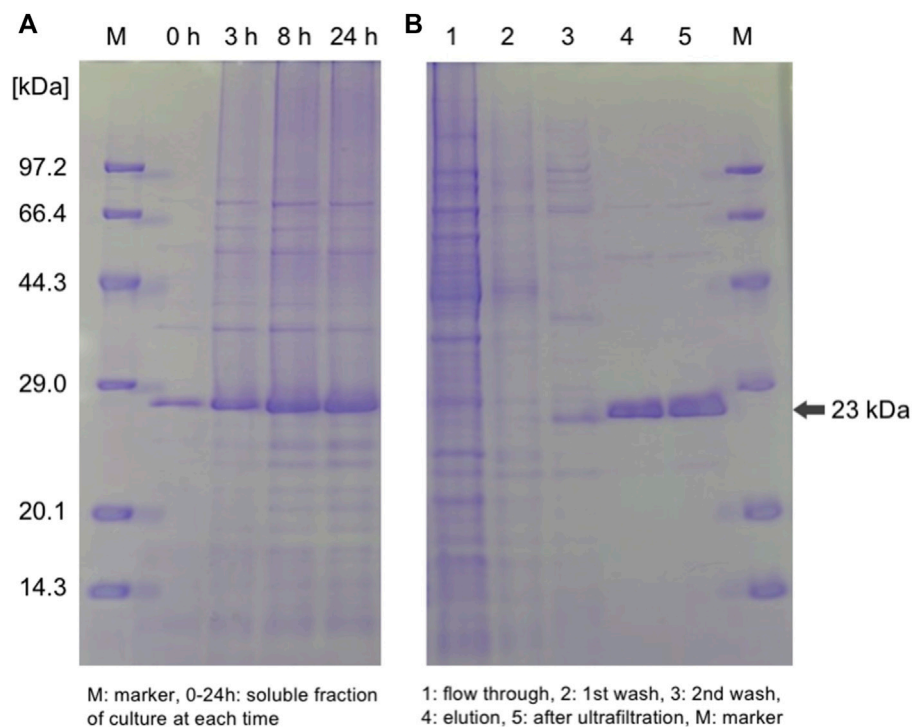


FIGURE 2

SDS-PAGE analysis of (A) expression and (B) purification of the target fusion protein CaBP-CBM.

induced carbonate precipitation (MICP). Urease-producing bacteria *Sporosarcina* sp. isolated from Miyazaki prefecture, Japan, were used for the experiments. The bacterial culture was prepared using an NH₄-YE medium by following the same procedure previously described (Nayanthara et al., 2019). The effect of the amount of CNF on sand solidification was investigated by mixing different amounts of CNF (0, 0.025, 0.05, 0.1, and 0.2 g) with Mikawa sand (40 g). Then, a 30-mL syringe was filled with the sand–CNF mixture in three layers, and each layer was subjected to 20 numbers of hammer blows. First, the bacterial suspension (16 mL, OD₆₀₀ = 1) was injected into the syringe and kept for 20 min for a better attachment of the bacteria into the sand particles. Next, the bacteria solution was drained out from the outlet, leaving the solution at 2 mm above the surface of the sand. The cementation solution (20 mL; 0.5 M urea, 0.5 M CaCl₂, 3 g/L nutrient broth) was added to the syringe and drained out from the outlet, leaving the solution at 2 mm above the surface of the sand to maintain saturation condition. Experiments were conducted in an incubator at 30°C for 14 days.

The bacteria suspension was injected into the sample two times, during the 1st day and the 7th day. After 14 days, the samples were removed from the syringe, and unconfined compressive strength (UCS) was determined by a needle penetration device (SH70, Maruto Testing Machine Company, Tokyo, Japan).

Similarly, experiments were conducted by adding additives. Samples were prepared with no additive, with CNF (0.025 g), with fusion protein (1.320 µg), and with both CNF and fusion protein.

3 Results and discussion

3.1 Gene construction and protein expression

Expression vectors pET-15b harboring the CaBP-CBM could be successfully prepared, and DNA sequencing of the gene was confirmed. According to the SDS-PAGE analysis (Figure 2A), CaBP-CBM was expressed successfully as a soluble protein in *E. coli*. A lower temperature (30°C) was used for the induction of protein expression by IPTG to avoid misfolding of proteins, which leads to formation of inclusion bodies (Nawarathna et al., 2021). As shown in Figure 2B, the expressed protein could be purified successfully using an IMAC Ni-charged column. By ultrafiltration, the purified protein was concentrated, and the buffer was replaced with Tris-HCl buffer (pH 9) since CBM3 has a higher binding affinity to cellulose at higher pH (Hong et al., 2007).

3.2 Solid-binding assay

We used different types of cellulosic materials, microcrystalline Avicel and CNF, and their morphologies were totally different as shown in Figure 3A. The binding ability of the fusion protein CaBP-CBM to these cellulosic materials was investigated. As shown in Figure 3B, over 90% of the fusion protein was adsorbed to CNF, while adsorption to Avicel was quite lower. CBM was well-known to be bound to cellulosic materials (Hong et al., 2007; Mwandira et al.,

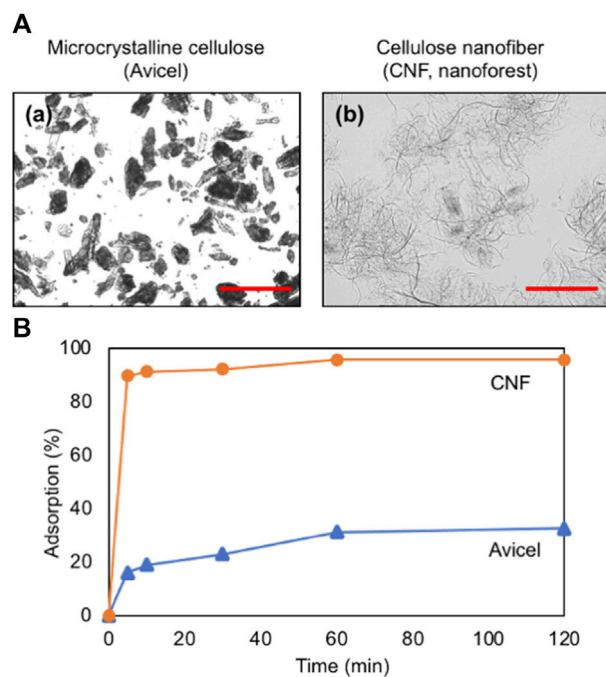


FIGURE 3

(A) Microscopic images of (a) microcrystalline cellulose (Avicel) and (b) cellulose nanofiber (CNF, nanoforest). Scale bars indicate 100 μm. (B) Adsorption profile of the fusion protein on Avicel and CNF.

2020; Togo et al., 2020), mostly through hydrophobic interaction (Chang et al., 2018). CBM3 is classified as type A, which has a surface-binding property, while type B and type C have glycan chain-binding and small sugar-binding properties (Boraston et al., 2004). Since CNF has a larger surface area, the binding ability of CBM was much higher than that of microcrystalline Avicel.

3.3 Effect of additives on CaCO₃ precipitation by using the EICP method

Biological CaCO₃ precipitation was conducted by using the EICP method with no cellulosic material, Avicel, and CNF in the presence or in the absence of the fusion protein. Figure 4 shows the SEM images of the precipitated CaCO₃ in each experimental condition. Rhombohedral-shaped crystals were formed with no additive (Figure 4A), and these crystals were found to be calcite by XRD analysis (Supplementary Figure S1). The addition of the fusion protein produced a different type of crystal of CaCO₃, that is, the agglomeration of small rhombohedral crystals and spherical- or flower-shaped crystals (Figure 4B). XRD analysis revealed that the crystals found in Figure 4B would be calcite and vaterite (Supplementary Figure S1). Calcite is the most stable type of polymorphism of CaCO₃ and is usually formed in urease-induced precipitation with different morphologies including rhombohedral, elongated, polyhedron, trigonal prism, or rod-shaped (Cheng et al., 2017; Xu et al., 2017; Hsu et al., 2018; Nawarathna et al., 2018). Flower-shaped vaterite crystals have been reported in previous papers (Navarro et al., 2007; Nawarathna et al., 2021). Organic materials promote the formation and stabilization of vaterite, which is the

metastable form of CaCO₃ polymorphism (Falini et al., 1998; Ouhenia et al., 2008). Supersaturation of the solution plays a role in the formation of vaterite crystals. Less stable CaCO₃ polymorphism such as vaterite is formed first at higher supersaturation (Lopez et al., 2001; Trushina et al., 2014) and is subsequently converted to more stable forms, such as calcite or aragonite. When the viscosity of the reaction mixture is higher, it encourages the enhancement of local ion concentration, and it leads to an increase in the supersaturation of the solution (Svenskaya et al., 2018). In the presence of the fusion protein, viscosity of the reaction mixture is comparatively higher than that of the reaction mixture without the fusion protein. Therefore, due to the presence of the fusion protein CaBP-CBM, the reaction mixture became supersaturated, resulting in the formation of vaterite crystals (Svenskaya et al., 2018). Furthermore, formation of vaterite crystals was accelerated under a higher concentration of the fusion protein due to the higher viscosity of the reaction mixture (Supplementary Figure S2).

With the addition of Avicel, the size and the number of rhombohedral crystals became smaller (Figure 4C), but it became bigger and increased by the combination of the fusion protein along with the formation of flower-shaped crystals (Figure 4D). Therefore, the fusion protein would contribute to the formation of calcite and vaterite in EICP-based CaCO₃ formation.

In the presence of CNF, smaller-sized rhombohedral crystals and agglomeration of rhombohedral calcite crystals were formed, as shown in Figure 4E. According to the SEM image, CNF has promoted the precipitation of the most stable form of CaCO₃ polymorphism. Previous research also found the formation of rhombohedral calcite crystals in the presence of cellulose fibers (Dalas et al., 2000; Vilela et al., 2010). Formation of a large number of small crystals without the growth

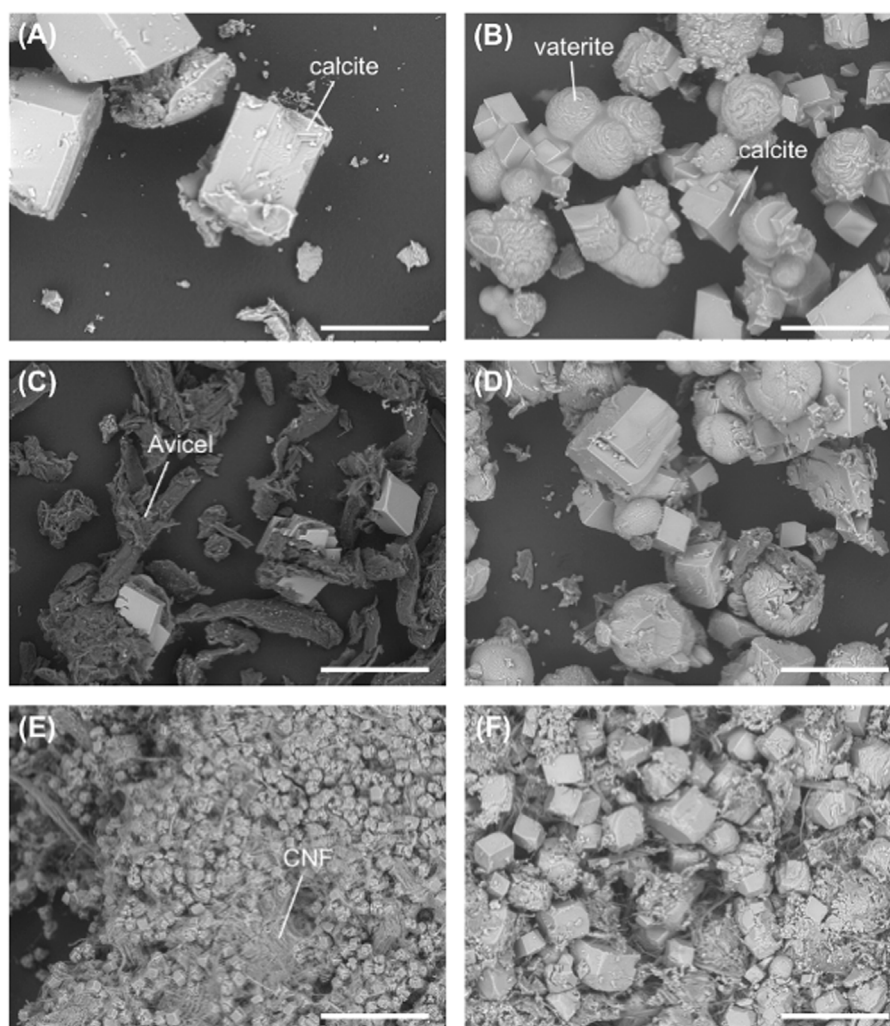


FIGURE 4

SEM images of the CaCO_3 precipitate with (A) no additive, (B) fusion protein, (C) Avicel, (D) Avicel + fusion protein, (E) CNF, and (F) CNF + fusion protein. Scale bars indicate 100 μm .

of the individual crystals would be mostly due to steric hindrance. Crystal growth of calcite could possibly be restricted by the limited space because of the tightly packed microenvironment of nanofibers. It is also confirmed by the results that clearly show the reduction of crystal size with the increase of CNF concentration (Supplementary Figure S3). With the addition of the fusion protein to the CNF system, the size of crystals became bigger (Figure 4F). The precipitate consisted of CaCO_3 crystals with different morphologies such as rhombohedral, polyhedron, and a small number of spherical crystals. The rhombohedral and polyhedron crystals would be calcite, and the spherical crystals should be vaterite. As mentioned above, organic materials assist in stabilizing the metastable form of CaCO_3 polymorphism. Polycrystalline particles appeared on the crystal surface, probably due to the absorption of the protein into the growing crystal faces. Even though space is limited, the fusion protein assisted to overcome it, leading to crystal growth by reducing the activation energy of nucleation to promote crystal growth. Amino acids have an ability of reducing the activation

energy of nucleation to promote crystal growth (Briegel and Seto, 2012). Previous studies revealed that most of proteins related to CaCO_3 biomineralization are richer in acidic amino acids than in basic amino acids (De Oliveira and Laursen, 1997; Sugawara et al., 2006). On the other hand, it was also reported that some basic amino acid residues in matrix proteins have assisted in CaCO_3 biomineralization (Jain et al., 2017). CaBP in the fusion protein shows positive charge because it is rich in basic amino acids such as lysine, histidine, and arginine residues (Nawarathna et al., 2021). Since the pH of the reaction mixture was around 9, arginine (dissociation constants/ $\text{pK}_a = 11$) was completely positively charged, and lysine ($\text{pK}_a = 9$) was partially charged, while histidine was almost electroneutral ($\text{pK}_a = 7$). Similarly, a higher amount of basic amino acids (positively charged) is present in CBM of the fusion protein. The presence of a higher amount of basic amino acids in the fusion protein could contribute to the promotion of CaCO_3 formation. Our previous research also reported a higher performance of CaCO_3 precipitation in recombinant protein composed of CaBP and chitin-binding domain (Nawarathna et al., 2021).

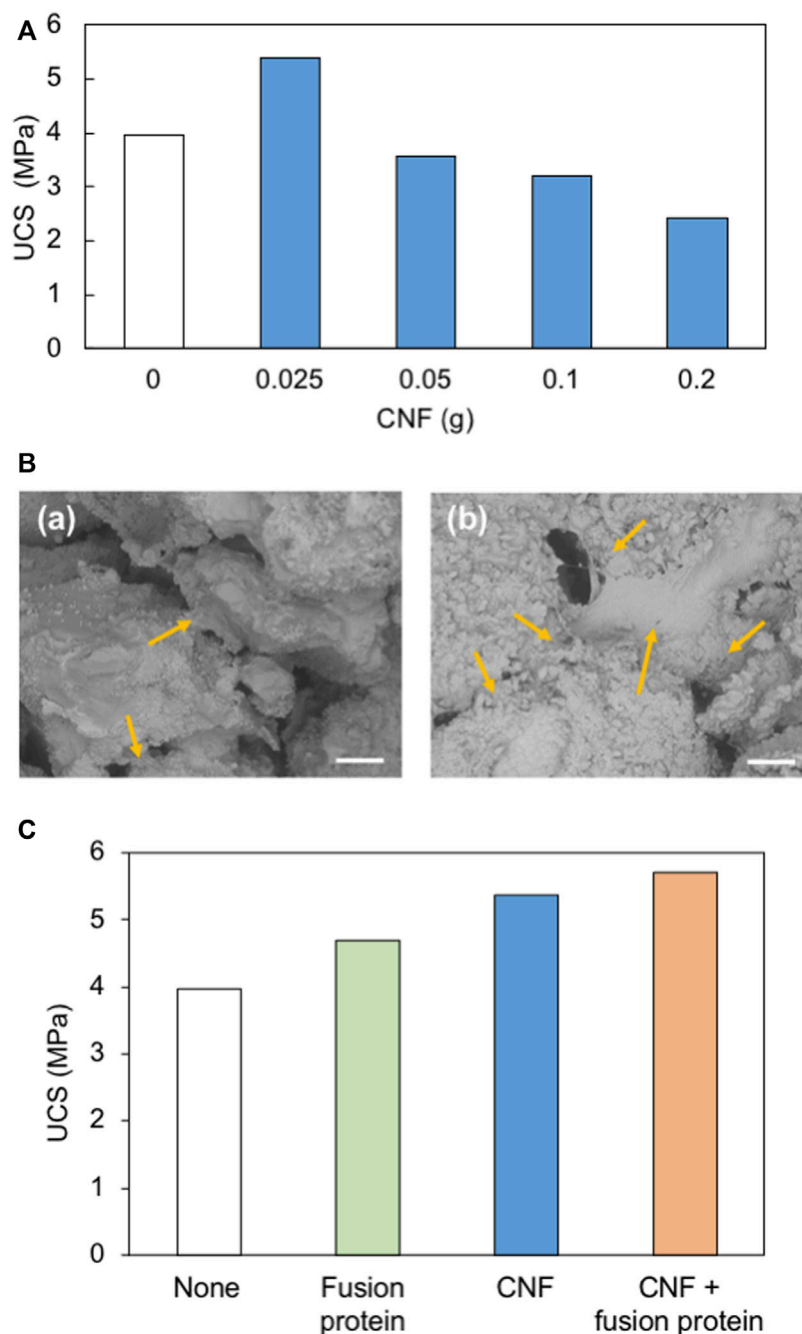


FIGURE 5

(A) Strength of biocemented sand specimens with different CNF content. (B) SEM images of solidified sand with (a) no additive and (b) CNF. Arrows show the connecting points between sand particles. Scale bars indicate 200 μm . (C) Comparison of the strength of biocemented sand with different additives.

3.4 Sand solidification

Sand solidification experiments were conducted with different amounts of CNF without the addition of the fusion protein. Sand was solidified by MICP by adding 0, 0.025, 0.05, 0.1, and 0.2 g of CNF. Figure 5A shows the UCS value obtained in the solidified samples with different CNF content, and the UCS results are based on the single-specimen test for each case. Compared with the control sample (0 g of CNF), the UCS of the biocemented specimen has increased by 35% by adding 0.025 g of CNF. As shown in Figure 4, a larger number of small

crystals were formed in the presence of CNF. A large number of smaller CaCO_3 crystals could be filled in the pore spaces between the soil particles effectively, resulting in the increase in strength of the specimen. In addition, CNF could work as a bridge to connect sand particles to provide higher strength, while the control sample without CNF showed less bonding between sand particles (Figure 5B). In the sand solidification process, pore spaces between sand particles should be filled appropriately, and an adequate bridge between sand particles should be formed to achieve a higher strength (Harkes et al., 2010). However, further increase of CNF content has led to a decrease in UCS,

and specimens show lower strength than the control sample without CNF. Addition of excessive fibers would just fill the pore space without cementation by CaCO_3 . Furthermore, bacteria cells would be attached to the fiber surface in the system with higher CNF content, resulting in the decrease in CaCO_3 formation, which is necessary for bridging sand particles. Because of the high contents of fiber, clogging could occur in the specimen, leading to a non-uniform distribution of bacteria and CaCO_3 formation, which could cause the weakness of the solidified sand. Previous works also found the reduction of the strength of biocemented soil with the increase of the fiber content (Li et al., 2016; Fang et al., 2020; Chen et al., 2021). Li et al. (2016) mentioned that optimum fiber content (polypropylene fiber) for biocemented sand is 0.2%–0.3%. Further increase of the fiber content will cause non-uniform distribution of bacteria, which leads to more precipitation on the fiber surface than on the contact points between the soil particles. Even though higher fiber content reduces the strength of the soil, it makes the sample more ductile (Chen et al., 2021). Generally, biocemented sand is a brittle material. Brittleness of the sample can be reduced, and ductility can be increased by adding fibers (Chen et al., 2021).

The effect of the type of additives (fusion protein, CNF, and combination of CNF and fusion protein) on sand solidification was investigated (Figure 5C). Samples with these additives show higher UCS values compared to the control sample (no additive). The strength of the sample has increased by 18%, 35%, and 44% with the addition of the fusion protein, CNF, and with both CNF and the fusion protein, respectively. The fusion protein has a greater contribution to the acceleration of CaCO_3 formation. At the same time, CNF acted as a bridge to combine soil particles. By the combination of these positive effects in solidification, the desirable solidification could be achieved in the CNF + fusion protein system.

4 Conclusion

A novel fusion protein, CaBP-CBM, was fabricated by the fusion of CaBP with CBM in order to promote efficient formation of CaCO_3 on the cellulose matrix. The developed recombinant protein showed a great influence on CaCO_3 crystallization and controlled the polymorphism of the crystals. Only calcite crystals were formed without any additives, while both calcite and vaterite crystals were formed with additives. The crystal's size also significantly increased with the fusion protein. The combination of the fusion protein and CNF considerably improved the biocementation process by providing higher strength in solidified sand. The developed fusion protein is a more sustainable approach to produce organic–inorganic hybrid composite materials for various industrial applications basically as a biocement, as a filler material for the paper industry, drug delivery, bio-medical applications (bone repair materials and artificial heart valves), and as functional materials for the water pre-treatment process.

References

- Arakaki, A., Shimizu, K., Oda, M., Sakamoto, T., Nishimura, T., and Kato, T. (2015). Biomineralization-inspired synthesis of functional organic/inorganic hybrid materials: organic molecular control of self-organization of hybrids. *Org. Biomol. Chem.* 13, 974–989. doi:10.1039/c4ob01796j
- Boraston, A. B., Bolam, D. N., Gilbert, H. J., and Davies, G. J. (2004). Carbohydrate-binding modules: fine-tuning polysaccharide recognition. *Biochem. J.* 382, 769–781. doi:10.1042/bj20040892
- Briegleb, C., and Seto, J. (2012). “Single amino acids as additives modulating CaCO_3 ,” in *Advanced topics in biomineralization*, BoD – Books on Demand, Norderstedt, Germany, 33–48.
- Chambers, A., Park, C., Baker, R. T. K., Rodriguez, N. M., Chen, P., Lin, J., et al. (1999). Polycationic peptides from diatom biosilica that direct silica nanosphere formation. *Science* 286, 1129–1132. doi:10.1126/science.286.5442.1129

Data availability statement

The datasets presented in this study can be found in online repositories. The names of the repository/repositories and accession number(s) can be found in the article/Supplementary Material.

Author contributions

TN: conceptualization and writing–original draft. JS: investigation, methodology, formal analysis, and writing–original draft. KN: conceptualization, funding acquisition, and writing–original draft. TK: conceptualization and writing–original draft. MS: formal analysis, investigation, methodology, and writing–original draft. CT: writing–review and editing. SK: writing–review and editing.

Funding

The author(s) declare financial support was received for the research, authorship, and/or publication of this article. This work was partly supported by JSPS KAKENHI Grant Numbers JP18H03395 and JP21H03627.

Conflict of interest

The authors declare that the research was conducted in the absence of any commercial or financial relationships that could be construed as a potential conflict of interest.

Publisher's note

All claims expressed in this article are solely those of the authors and do not necessarily represent those of their affiliated organizations, or those of the publisher, the editors, and the reviewers. Any product that may be evaluated in this article, or claim that may be made by its manufacturer, is not guaranteed or endorsed by the publisher.

Supplementary material

The Supplementary Material for this article can be found online at: <https://www.frontiersin.org/articles/10.3389/fbuil.2023.1305003/full#supplementary-material>

- Chang, F., Xue, S., Xie, X., Fang, W., Fang, Z., and Xiao, Y. (2018). Carbohydrate-binding module assisted purification and immobilization of β -glucosidase onto cellulose and application in hydrolysis of soybean isoflavone glycosides. *J. Biosci. Bioeng.* 125, 185–191. doi:10.1016/j.jbiosc.2017.09.001
- Chen, M., Gowthaman, S., Nakashima, K., Komatsu, S., Kawasaki, S., and Tian, H. (2021). Red, green, and blue light-emitting carbon dots prepared from gallic acid for white light-emitting diode applications. *Materials* 4, 14–18. doi:10.1039/d1na00730k
- Cheng, L., Shahin, M. A., and Mujah, D. (2017). Influence of key environmental conditions on microbially induced cementation for soil stabilization. *J. Geotech. Geoenviron.* 143, 04016083–04016091. doi:10.1061/(asce)gt.1943-5606.0001586
- Dalas, E., Klepetsanis, P. G., and Koutsoukos, P. G. (2000). Calcium carbonate deposition on cellulose. *J. Colloid Interface Sci.* 224, 56–62. doi:10.1006/jcis.1999.6670
- DeJong, J. T., Fritzes, M. B., and Nusslein, K. (2006). Microbially induced cementation to control sand response to undrained shear. *J. Geotech. Geoenviron. Eng.* 132, 1381–1392. doi:10.1061/(asce)1090-0241(2006)132:11(1381)
- De Oliveira, D. B., and Laursen, R. A. (1997). Control of calcite crystal morphology by a peptide designed to bind to a specific surface. *J. Am. Chem. Soc.* 119, 10627–10631. doi:10.1021/ja972270w
- Dorozhkin, S. V., and Epple, M. (2002). Biological and medical significance of calcium phosphates. *Angew. Chem. Int. Ed.* 41, 3130–3146. doi:10.1002/1521-3773(20020902)41:17<3130::aid-anie3130>3.0.co;2-1
- Ezquerro, C. S., Laspalas, M., Aznar, J. M. G., and Minana, C. C. (2023). Monitoring interactions through molecular dynamics simulations: effect of calcium carbonate on the mechanical properties of cellulose composites. *Cellulose* 30, 705–726. doi:10.1007/s10570-022-04902-1
- Falini, G., Fermiani, S., Gazzano, M., and Ripamonti, A. (1998). Oriented crystallization of vaterite in collagenous matrices. *Chem. Eur. J.* 4, 1048–1052. doi:10.1002/(sici)1521-3765(19980615)4:6<1048::aid-chem1048>3.0.co;2-u
- Fang, X., Yang, Y., Chen, Z., Liu, H., Xiao, Y., and Shen, C. (2020). Influence of fiber content and length on engineering properties of micp-treated coral sand. *Geomicrobiol. J.* 37, 582–594. doi:10.1080/01490451.2020.1743392
- Gowthaman, S., Mitsuyama, S., Nakashima, K., Komatsu, M., and Kawasaki, S. (2019). Biogeotechnical approach for slope soil stabilization using locally isolated bacteria and inexpensive low-grade chemicals: a feasibility study on Hokkaido expressway soil, Japan. *Jpn. Soils Found.* 59, 484–499. doi:10.1016/j.sandf.2018.12.010
- Hamdan, N., Zhao, Z., Mujica, M., Kavazanjian, E., and He, X. (2016). Hydrogel-assisted enzyme-induced carbonate mineral precipitation. *J. Mater. Civ. Eng.* 28, 28. doi:10.1061/(asce)mt.1943-5533.0001604
- Harkes, M. P., Paassen, L. A. V., Booster, J. L., Whiffin, V. S., and Loosdrecht, M. C. M. V. (2010). Fixation and distribution of bacterial activity in sand to induce carbonate precipitation for ground reinforcement. *Ecol. Eng.* 36, 112–117. doi:10.1016/j.ecoleng.2009.01.004
- Hong, J., Ye, X., and Zhang, Y. H. P. (2007). Quantitative determination of cellulose accessibility to cellulase based on adsorption of a nonhydrolytic fusion protein containing CBM and GFP with its applications. *Langmuir* 23, 12535–12540. doi:10.1021/la7025686
- Hsu, C. M., Huang, Y. H., Nimje, V. R., Lee, W. C., Chen, H. J., Kuo, Y. H., et al. (2018). Comparative study on the sand bioconsolidation through calcium carbonate precipitation by *Sporosarcina pasteurii* and *Bacillus subtilis*. *Crystals* 8, 189–204. doi:10.3390/cryst8050189
- Inoue, H., Ozaki, N., and Nagasawa, H. (2014). Purification and structural determination of a phosphorylated peptide with anti-calcification and chitin binding activities in the exoskeleton of crayfish, *Procambarus clarkii*. *Biosci. Biotechnol. Biochem.* 65, 1840–1848. doi:10.1271/bbb.65.1840
- Jackson, A. P., Vincent, J. F. V., and Turner, R. M. (1990). Comparison of nacre with other ceramic composites. *J. Mater. Sci.* 25, 3173–3178. doi:10.1007/bf00587670
- Jain, G., Pendola, M., Huang, Y. C., Gebauer, D., and Evans, J. S. A. (2017). A model sea urchin spicule matrix protein, rSpSM50, is a hydrogelator that modifies and organizes the mineralization process. *Biochemistry* 56, 2663–2675. doi:10.1021/acs.biochem.7b00083
- Jin, C., Zhao, J., Pu, J., Liu, X., and Li, J. (2019). Hichin, a chitin binding protein is essential for the self-assembly of organic frameworks and calcium carbonate during shell formation. *Int. J. Biol. Macromol.* 135, 745–751. doi:10.1016/j.jbiomac.2019.05.205
- Klemm, D., Heublein, B., Fink, H.-P., and Bohn, A. (2005). Cellulose: fascinating biopolymer and sustainable raw material. *Angew. Chem. Int. Ed.* 44, 3358–3393. doi:10.1002/anie.200460587
- Kramar, A., and González-Benito, F. J. (2022). Cellulose-based nanofibers processing techniques and methods based on bottom-up approach - a review. *Polymers* 14, 286–335. doi:10.3390/polym14020286
- Kuo, D., Nishimura, T., Kajiyama, S., and Kato, T. (2018). Bioinspired environmentally friendly amorphous CaCO₃-based transparent composites comprising cellulose nanofibers. *ACS Omega* 3, 12722–12729. doi:10.1021/acsomega.8b02014
- Li, M., Li, L., Ogbonnaya, U., Wen, K., Tian, A., and Amini, F. (2016). Influence of fiber addition on mechanical properties of MICP-treated sand. *J. Mater. Civ. Eng.* 28, 1–10. doi:10.1061/(asce)mt.1943-5533.0001442
- Lopez, C. J., Caballero, E., Huertas, F. J., and Romanek, C. S. (2001). Chemical, mineralogical and isotope behavior, and phase transformation during the precipitation of calcium carbonate minerals from intermediate ionic solution at 25°C. *Geochim. Cosmochim. Acta* 65, 3219–3231. doi:10.1016/s0016-7037(01)00672-x
- Maroney, M. J., and Ciarli, S. (2014). Nonredox nickel enzymes. *Chem. Rev.* 114, 4206–4228. doi:10.1021/cr4004488
- Montagnani, C., Marie, B., Marin, F., Belliard, C., Riquet, F., Tayale, A., et al. (2011). Pmarg-Pearlin is a matrix protein involved in nacre framework formation in the pearl oyster *Pinctada margaritifera*. *Chem. Bio. Chem.* 12, 2033–2043. doi:10.1002/cbic.201100216
- Mwandira, W., Nakashima, K., Togo, Y., Sato, T., and Kawasaki, S. (2020). Cellulose-metallothionein biosorbent for removal of Pb(II) and Zn(II) from polluted water. *Chemosphere* 246, 125733. doi:10.1016/j.chemosphere.2019.125733
- Nakayama, S., Suzuki, M., Endo, H., Iimura, K., Kinoshita, S., Watabe, S., et al. (2013). Identification and characterization of a matrix protein (ppp-10) in the periostracum of the pearl oyster, *Pinctada Fucata*. *FEBS Open Bio* 3, 421–427. doi:10.1016/j.fob.2013.10.001
- Navarro, C. R., Lopez, C. J., Navarro, A. R., Munoz, M. T. G., and Gallego, M. R. (2007). Bacterially mediated mineralization of vaterite. *Geochim. Cosmochim. Acta* 71, 1197–1213. doi:10.1016/j.gca.2006.11.031
- Nawarathna, T. H. K., Nakashima, K., Fujita, M., Takatsu, M., and Kawasaki, S. (2018). Effects of cationic polypeptide on CaCO₃ crystallization and sand solidification by microbial-induced carbonate precipitation. *ACS Sustain. Chem. Eng.* 6, 10315–10322. doi:10.1021/acssuschemeng.8b01658
- Nawarathna, T. H. K., Nakashima, K., Kawabe, T., Mwandira, W., Kurumisawa, K., and Kawasaki, S. (2021). Artificial fusion protein to facilitate calcium carbonate mineralization on insoluble polysaccharide for efficient biocementation. *ACS Sustain. Chem. Eng.* 9, 11493–11502. doi:10.1021/acssuschemeng.1c03730
- Nawarathna, T. H. K., Nakashima, K., and Kawasaki, S. (2019). Chitosan enhances calcium carbonate precipitation and solidification mediated by bacteria. *Int. J. Biol. Macromol.* 133, 867–874. doi:10.1016/j.jbiomac.2019.04.172
- Nayanthara, P. G. N., Dassanayake, A. B. N., Nakashima, K., and Kawasaki, S. (2019). Biocementation of Sri Lankan beach sand using locally isolated bacteria: a baseline study on the effect of segregated culture media. *Int. J. GEOMATE* 17, 55–62. doi:10.21660/2019.63.8238
- Ouhenia, S., Chateigner, D., Belkhir, M. A., Guilmeau, E., and Krauss, C. (2008). Synthesis of calcium carbonate polymorphs in the presence of polyacrylic acid. *J. Cryst. Growth* 310, 2832–2841. doi:10.1016/j.jcrysgro.2008.02.006
- Rebers, J. E., and Riddiford, L. M. (1988). Structure and expression of a manduca sexta larval cuticle gene homologous to Drosophila cuticle genes. *J. Mol. Biol.* 203, 411–423. doi:10.1016/0022-2836(88)90009-5
- Saito, T., Oaki, Y., Nishimura, T., Isogai, A., and Kato, K. (2014). Bioinspired stiff and flexible composites of nanocellulose-reinforced amorphous CaCO₃. *Mater. Horiz.* 1, 321–325. doi:10.1039/c3mh00134b
- Sarikaya, M., Tamerler, C., Jen, A. K., Schulten, K., and Baneyx, F. (2003). Molecular biomimetics: nanotechnology through biology. *Nat. Mater.* 2, 577–585. doi:10.1038/nmat964
- Shi, R.-J., Lang, J.-Q., Wang, T., Zhou, N., and Ma, M.-G. (2022). Fabrication, properties, and biomedical applications of calcium-containing cellulose-based composites. *Front. Bioeng. Biotechnol.* 10, 937266–937313. doi:10.3389/fbioe.2022.937266
- Stephen, W., and Lia, A. (1997). Design strategies in mineralized biological materials. *J. Mater. Chem.* 7, 689–702. doi:10.1039/a604512j
- Sudo, S., Fujikawa, T., Ohkubo, T., Sakaguchi, K., Tanaka, M., and Nakashima, K. (1997). Structures of mollusc shell framework proteins. *Nature* 387, 563–564. doi:10.1038/42391
- Sugawara, A., Nishimura, T., Yamamoto, Y., Inoue, H., Nagasawa, H., and Kato, T. (2006). Self-organization of oriented calcium carbonate/polymer composites: effects of a matrix peptide isolated from the exoskeleton of a crayfish. *Angew. Chem. Int. Ed.* 45, 2876–2879. doi:10.1002/anie.200503800
- Suzuki, M., Saruwatari, K., Kogure, T., Yamamoto, Y., Nishimura, T., Kato, T., et al. (2009). An acidic matrix protein, Pif, is a key macromolecule for nacre formation. *Science* 325, 1388–1390. doi:10.1126/science.1173793
- Svenskaya, Y. I., Fattah, H., Inozemtseva, O. A., Ivanova, A. G., Shtykov, S. N., Gorin, D. A., et al. (2018). Key parameters for size- and shape-controlled synthesis of vaterite particles. *Cryst. Growth Des.* 18, 331–337. doi:10.1021/acs.cgd.7b01328
- Togo, Y., Nakashima, K., Mwandira, W., and Kawasaki, S. (2020). A novel metal adsorbent composed of a hexa-histidine tag and a carbohydrate-binding module on cellulose. *Anal. Sci.* 36, 459–464. doi:10.2116/analsci.19p356
- Trushina, D. B., Bukreeva, T. V., Kovalchuk, M. V., and Antipina, M. N. (2014). CaCO₃ vaterite microparticles for biomedical and personal care applications. *Mater. Sci. Eng. C* 45, 644–658. doi:10.1016/j.msec.2014.04.050
- Vilela, C., Freire, C. S. R., Marques, P. A. A. P., Trindade, T., Neto, C. P., and Fardim, P. (2010). Synthesis and characterization of new CaCO₃/cellulose nanocomposites prepared by controlled hydrolysis of dimethylcarbonate. *Carbohydr. Polym.* 79, 1150–1156. doi:10.1016/j.carbpol.2009.10.056
- Whiffin, V. S., Van Paassen, L. A., and Harkes, M. P. (2007). Microbial carbonate precipitation as a soil improvement technique. *Geomicrobiol. J.* 24, 417–423. doi:10.1080/01490450701436505
- Xu, G., Tang, Y., Lian, J., Yan, Y., and Fu, D. (2017). Mineralization process of biocemented sand and impact of bacteria and calcium ions concentrations on crystal morphology. *Adv. Mater. Sci. Eng.* 2017, 1–13. doi:10.1155/2017/5301385
- Zhao, Z., Hamdan, N., Shen, L., Nan, H., Almajed, A., Kavazanjian, E., et al. (2016). Biomimetic hydrogel composites for soil stabilization and contaminant mitigation. *Environ. Sci. Technol.* 50, 12401–12410. doi:10.1021/acs.est.6b01285